

An Auto-Locked Diode Laser System for Precision Metrology

H. C. Beica^a, A. Carew^b, A. Vorozcovs^c, P. Dowling^d, A. Pouliot^e, G. Singh^f, and A. Kumarakrishnan^g

^aDepartment of Physics and Astronomy, York University, Toronto, Ontario, M3J 1P3, Canada
^{b, c, d, e, f, g} Department of Physics and Astronomy, York University, Toronto, Ontario, M3J 1P3, Canada

ABSTRACT

We describe a diode laser system for precision metrology that relies on adaptations of a well-known design based on optical feedback from an interference filter. The laser head operates with an interchangeable baseplate, which allows for single-mode performance at two distinct wavelengths of 633 nm and 780 nm. Frequency drifts are effectively suppressed by using a vacuum-sealed laser head, thereby allowing the laser frequency to be stabilized on time-scales of several hours. By using a digital auto-lock controller, the laser frequency can be stabilized with respect to selected iodine and rubidium spectral lines. The controller can be programmed to use a pattern-matching algorithm or generate first- and third-derivative error signals for peak locking. Beat note characterization has demonstrated a short-term linewidth of ~ 2 MHz and an Allan deviation of 3.5×10^{-9} for a measurement time $\tau = 500$ s. The laser characteristics have also enabled high-precision gravity measurements with accuracies of a few parts-per-billion (ppb).

Keywords: Auto-lock controller

1. INTRODUCTION

One of the main challenges in precision spectroscopy using diode lasers is the design of a suitable external cavity to narrow the laser linewidth using optical feedback, and achieve precise control of tuning and locking the laser frequency with reference to spectral lines. Well-known designs have used combinations of gratings, etalons, and beam-splitters to provide optical feedback to the laser diode.¹⁻⁷ In the widely-used Littrow design, scanning the laser frequency with a piezo-mounted grating changes the optical feedback as well as the length of the external cavity. This disadvantage can be overcome by positioning the grating at a carefully chosen pivot point,⁵ whereas the overall stability of the cavity can be improved using a monolithic design.⁷ The limited mode-hop-free tuning range of the system can be significantly extended by synchronous scanning of the current and the grating using a feed-forward circuit. In comparison, interference filter (IF)-stabilized diode lasers have the advantage that the IF used for wavelength selection is separate from the piezo-mounted mirror which changes the length of the laser cavity. This IF design also prevents distortions of the spatial beam profile, thereby making it potentially easier to achieve mode-hop-free tuning over the free-spectral range of the cavity.

Previous work^{3,4} showed that the IF design exhibited a narrow linewidth (tens of kHz) and a tuning range of several nanometers achieved by changing the incidence angle of the filter. Recent work⁵ showed the spectral resolution of the laser in the 780-nm band and reduced sensitivity to acoustic noise. In our work, we demonstrate operation at two distinct wavelengths (633 nm and 780 nm) using the same laser head design and an auto-lock controller. The wavelength changes are achieved by changing the optics kit and laser diode. By studying rubidium and iodine hyperfine spectra, we demonstrate suppression of pressure-induced frequency drifts, leading to long-term lock stability. The lasers are characterized using measurements of linewidth and Allan deviation. Applications to precision metrology are demonstrated through accurate measurements of gravitational acceleration.

Further author information: (Send correspondence to H.C.B.)
H.C.B.: E-mail: hermina@yorku.ca, Telephone: 1 416 736 2100
A.K.: E-mail: akumar@yorku.ca, Telephone: 1 416 736 2100

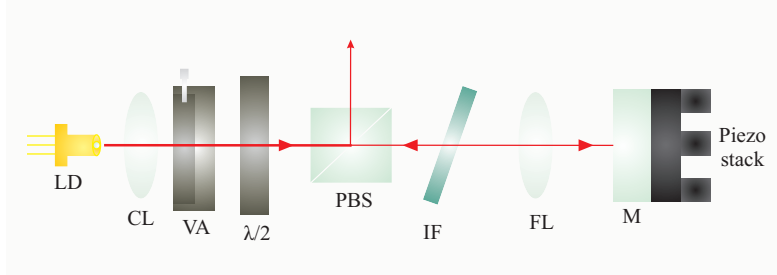


Figure 1: Schematic of IF laser design. The optical elements are: LD - laser diode, CL - collimating lens, VA - variable aperture, $\lambda/2$ - half wave-plate, PBS - polarizing beam splitter, IF - interference filter, FL - focusing lens, M - mirror.

2. IF LASER DESIGN

We now outline the basic features of our adaptations of the IF laser head design. Fig. 1 shows a schematic of the laser head. Light from the laser diode is collimated and aligned through a half wave-plate and a polarization-sensitive beam splitter. About 85% of the laser power is output-coupled, while the horizontally-polarized transmitted beam ($\sim 15\%$) passes through an IF filter with a transmission full width at half maximum (FWHM) of 0.3 nm. The selected wavelengths are optically fed back into the laser diode using a ‘cat’s eye’ reflector consisting of a piezo-mounted mirror placed at the focal length of a lens. The external cavity length, measured from the laser diode to the retro-reflecting mirror, is 10 cm. The output of the laser cavity is the vertically-polarized reflection from the beam splitter. All the optical elements of the laser cavity are mounted on a compact, temperature-stabilized base-plate. This base-plate can be easily interchanged to allow the laser to operate within a desired wavelength range. A variable aperture mounted near the laser diode is used to spatially filter unwanted components of the feedback light, such as stray reflections.

Even if the laser current and temperature are well controlled, a key challenge for effective frequency stabilization is to limit laser frequency drifts caused by ambient pressure variations. These pressure changes (~ 1 MHz/minute) can lead to frequency drifts that exceed the lock range of the controller on time-scales of a few minutes. To address this limitation and suppress the pressure drifts, the laser cavity has been designed with a viton seal, so that it can be evacuated to ~ 50 mTorr, and sealed for several months. Since the pump-out changes the index of refraction inside the laser cavity, the IF needs to be adjusted to optimize the feedback at the vacuum wavelength. Here, adjustments to the filter angle are achieved from outside the laser cavity by using a gear mechanism attached to a vacuum feed-through. The gear ratio of 18:1 allows the angular position of the filter to be adjusted to within 1 mrad. An electrical vacuum feed-through enables the current, temperature, and piezo voltage to be controlled from outside the laser cavity, and allows the pressure inside the cavity to be monitored.

The laser frequency of our 633-nm and 780-nm lasers can be stabilized to respective iodine and rubidium hyperfine spectral features by using a digital auto-lock controller. The auto-lock controller comprises of a low-cost, single-board computer with A/D and D/A capability that acts as a specialized lock-in amplifier. It is also responsible for unattended start-up of the laser and laser mode monitoring functions. In order to bring the laser to the desired spectral location (frequency) from a cold-start condition, the controller performs pattern matching between Doppler-free peaks obtained by scanning the laser frequency and reference peaks stored in the processor’s memory. The incoming spectral signals are compared with the reference waveforms using a sliding correlation algorithm, which determines the control voltage required for adjusting the laser frequency to the desired lock point. The system has a scan amplitude of less than 1 MHz when locked, and it can re-lock for frequency drifts of up to 10 GHz without human intervention. In general, the controller uses a pattern-matching algorithm to lock to rubidium hyperfine lines. For locking to iodine lines, the digitizing signal processor in the controller generates first- and third-derivative error signals.

3. RESULTS AND DISCUSSION

Laser characterization of the 633-nm and 780-nm system is carried out using a dual-pass saturated absorption spectrometer,⁸ a Fabry-Perot interferometer (free-spectral range of 10 GHz), and a wavemeter (resolution of 50 MHz), as shown in Fig. 2. The Fabry-Perot interferometer and the wavemeter are used to monitor the single-mode behaviour of the laser and the absolute wavelength, respectively.

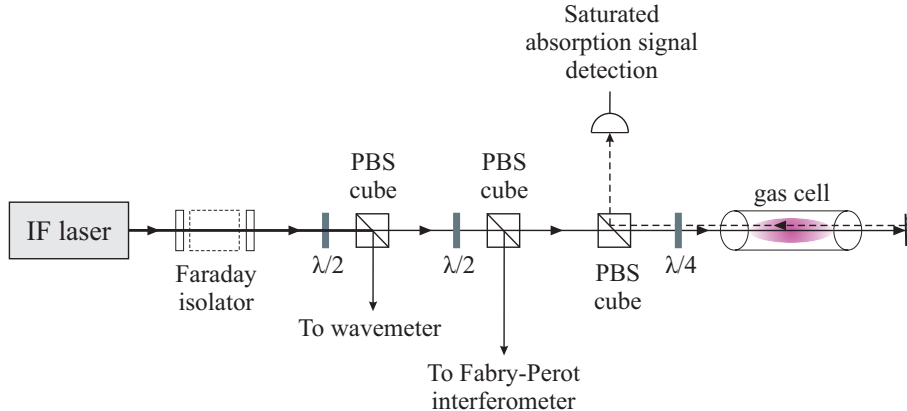


Figure 2: Dual-pass saturated absorption set-up for iodine and rubidium spectroscopy.

In the saturated absorption set-up, a relatively strong pump beam is circularly-polarized and sent through an iodine or rubidium vapour cell. This beam is then retro-reflected as a weakened probe beam. The counter-propagating probe beam is separated from the pump by a polarizing beam splitter, and the probe absorption is recorded on a photodiode. Figs. 3(a), (b), and (c) show absorption spectra of the P(33)6-3 iodine lines.

Laser frequency stabilization was achieved on the basis of third-derivative signals of hyperfine transitions in the P(33)6-3 branch in iodine. Fig. 4(a) shows the correction signal over a range of approximately 100 MHz. A Gaussian fit to the histogram of the corresponding error signal in the figure shows a lock stability of 0.5 MHz over a period of 3 hours. This data was acquired with a feed-back time constant of approximately 1 second. Under these conditions, the laser can be frequency stabilized over extended periods of time (several hours), thereby making it well-suited for precision measurements. Fig. 4(b) shows similar data to (a), with the laser cavity pumped out to ~ 50 mTorr. The fluctuations in the correction voltage are reduced by a factor of 10, with the pressure-induced drifts highly suppressed and uncorrelated with the variations in air pressure outside the cavity. Under these conditions, the lock durations are typically extended. However, the error signal has a lock stability of 0.9 MHz, suggesting that the pump-out procedure potentially induces virtual leaks that result in cavity vibrations. We expect to improve the lock stability by modifying our design to include pressure-release channels in different optical components. This laser configuration proved to be well-suited for measurements of the absolute value of the gravitational acceleration \mathbf{g} using a falling corner cube gravimeter (Scintrex FG5X).⁹ The measured value of \mathbf{g} had an accuracy of 3 parts-per-billion, with residuals that were smaller than those obtained using an industrial standard (iodine-stabilized He-Ne laser).

By interchanging the base-plate and laser diode inside the laser head, we obtained similar absorption spectra in rubidium, as shown in Fig. 5.

Similar lock data are shown in Fig. 6(a) and (b). For this data, the feedback corrections were generated using a simplified digital feedback algorithm. The laser frequency was scanned across resonance by applying a triangular waveform (typical amplitude of 30 MHz) from a function generator. The Doppler-free absorption was processed by a data card (48,000 samples/s with 16-bit resolution), which computed feedback corrections based on frequency offsets with respect to the line center. The corrections were sent from the data card into the function generator through a GPIB connection. The frequency corrections were computed on the basis of the position of a Doppler-free peak (the lock point) with respect to the center of the ramp voltage. A positive or negative correction was applied if the peak drifted from the center point. The time constant of the feedback

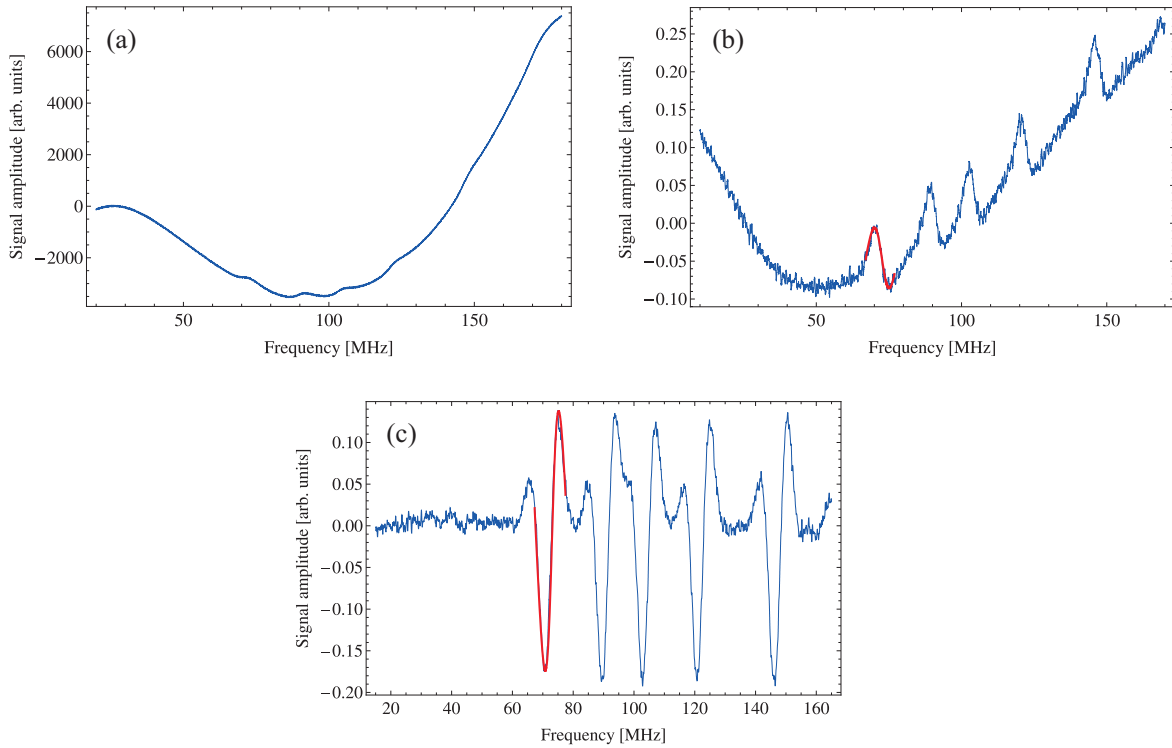


Figure 3: (a) AC-coupled signal showing the Doppler-broadened spectrum of the P(33)6-3 branch in iodine at 633 nm. (b) First derivative of the photodiode signal in (a). (c) Third derivative of the photodiode signal in (a).

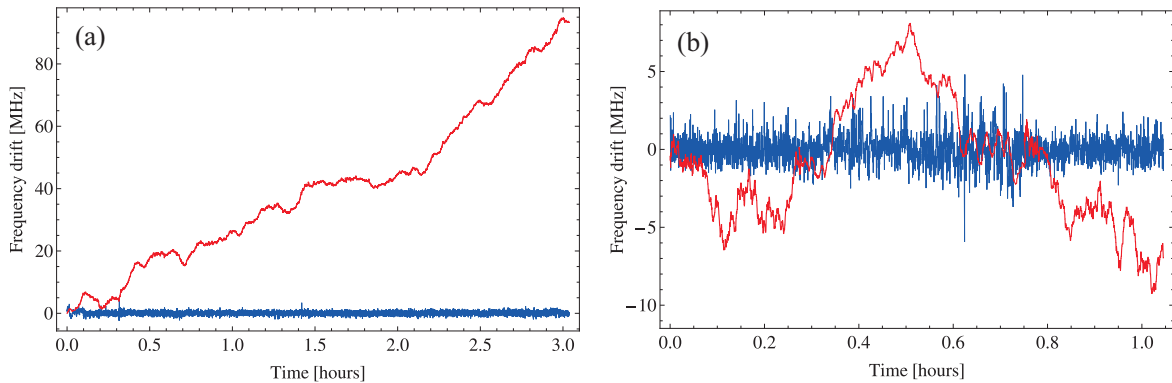


Figure 4: (a) Plot of the lock error signal (blue) and correction signal (red) with the laser cavity in air. For this data set, the laser frequency was locked on the basis of the third-derivative signals in iodine shown in Fig. 3(c). (b) Plot of the lock error signal (blue) and correction signal (red) with the laser cavity pumped out to ~ 50 mTorr. Just like the signals in part (a), the lock was generated from third-derivative signals in iodine.

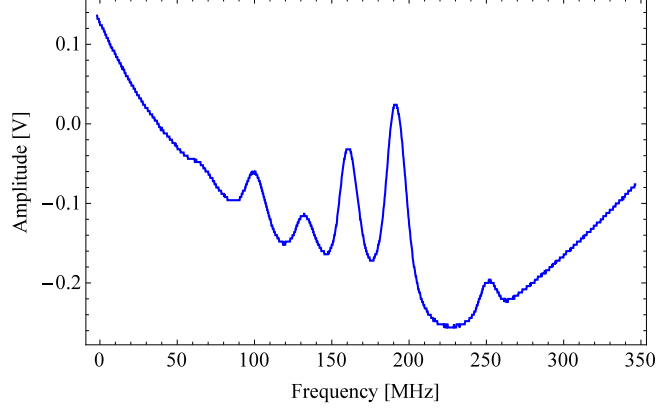


Figure 5: AC-coupled signal showing hyperfine spectrum of the $5^2S_{1/2} F = 3 \rightarrow 5^2P_{3/2} F' = 2, 3, 4$ transition in ^{85}Rb .

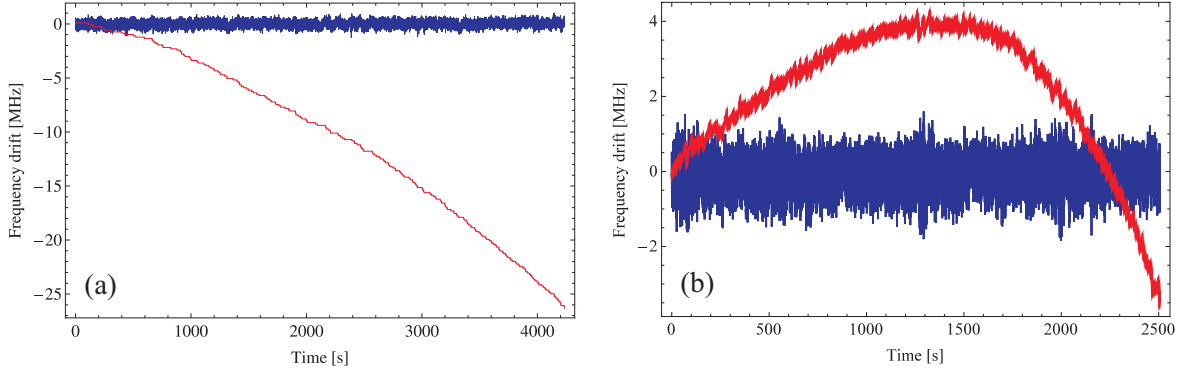


Figure 6: (a) Plot of the lock error signal (blue) and correction signal (red) with the laser cavity hermetically sealed. For this data set, the laser frequency was locked to the $5^2S_{1/2} F = 3 \rightarrow 5^2P_{3/2} F' = 4$ peak in ^{85}Rb . (b) Plot of the lock error signal (blue) and correction signal (red) with the laser cavity pumped out to ~ 50 mTorr. Once again, the laser frequency was locked to the $5^2S_{1/2} F = 3 \rightarrow 5^2P_{3/2} F' = 4$ peak in ^{85}Rb .

loop was inferred to be 1 second. The typical lock stability was 0.7 MHz with the cavity in air, as shown in Fig. 6(a). The data was then repeated with the laser cavity pumped to ~ 50 mTorr, resulting in a lock stability of 0.9 MHz over time-scales of approximately one hour, as shown in Fig. 6(b). These results were qualitatively similar to the performance of the 633-nm laser systems.

The laser linewidth was characterized by acquiring a 60-90 MHz beat note on a time-scale of 50 ms. For the 780-nm systems, the lasers were tuned to neighbouring hyperfine transitions within the same Doppler group in ^{85}Rb . The Fourier transform of the beat signal was obtained using a spectrum analyser. Since the measurement was dominated by current noise, a Gaussian fit was used to infer the laser linewidth. We obtained a linewidth of 2.9 MHz with hermetically-sealed cavities, and a reduced linewidth of 2.1 MHz at pressures of ~ 50 mTorr. The small reduction in the linewidth suggests that the pump-out procedure reduced some sources of vibrations contributing to line-broadening. For the 633-nm systems, the corresponding linewidth was found to be 2.1 MHz with hermetically-sealed cavities, and 1.5 MHz for pumped-out laser cavities.

Preliminary Allan deviation measurements of beat note and lock stability were carried out for one-hour lock durations without the use of vibration-isolation platforms. The minimum Allan deviation of the beat note was determined to be 3.5×10^{-9} for a measurement time $\tau = 500$ s with the laser cavities hermetically sealed, and 4×10^{-9} for $\tau = 1000$ s with the cavities pumped out to ~ 50 mTorr. These results also suggest that the pump-out procedure induces instabilities inside the laser cavity. However, the time at which the minimum Allan

deviations are measured with our lasers is noteworthy, since we used a time constant of 1 s, whereas typical Allan deviation plots for vibration-isolated diode lasers range from 10^{-10} to 10^{-11} at $\tau = 1$ s with time constants of 1 ms.^{10,11} We expect to attain comparable values by reducing current noise, improving the vibration isolation, and applying feedback corrections on faster time-scales.

4. CONCLUSIONS

We have presented an improved vacuum-sealed, auto-locked, IF-stabilized diode laser system that is capable of operating at both 633 nm and 780 nm. The measured laser linewidth is suitable for performing spectroscopy in iodine and rubidium, and precise measurements of the local gravitational acceleration \mathbf{g} . The auto-locking technique is sufficiently general that different control algorithms can be programmed for locking to spectra in rubidium and iodine. The interchangeable base-plate design allows the laser head to be configured for the desired wavelength range. Vacuum-sealing the laser head has suppressed the effects of pressure variations by a factor of 10, and led to laser locking over extended durations of time. Under these conditions, the laser drifts are sufficiently minimal that the feedback loop can operate with time constants of ~ 1 s.

REFERENCES

- [1] Young, L., Hill, W. T., Sibener, S. J., Price, S. D., Tanner, C. E., Wieman, C. E., and Leone, S. R., “Precision lifetime measurements of Cs $6p\ ^2P_{1/2}$ and $6p\ ^2P_{3/2}$ levels by single-photon counting,” *Phys. Rev. A* **50**, 2174–2181 (1994).
- [2] Ricci, L., Weidemuller, M., Esslinger, T., Hemmerich, A., Zimmermann, C., Vuletic, V., Konig, W., and Hansch, T. W., “A compact grating-stabilized diode laser system for atomic physics,” *Opt. Comm.* **117**, 541–549 (1995).
- [3] Baillard, X., Gauguier, A., Bize, S., Lemonde, P., Laurent, P., Clairon, A., and Rosenbusch, P., “Interference-filter-stabilized external-cavity diode lasers,” *Opt. Comm.* **266**, 609–613 (2006).
- [4] Gilowski, M., Schubert, C., Zaiser, M., Herr, W., Wubbena, T., Wendrich, T., Muller, T., Rasel, E. M., and Ertmer, W., “Narrow bandwidth interference filter-stabilized diode laser systems for the manipulation of neutral atoms,” *Opt. Comm.* **280**, 443–447 (2007).
- [5] Saliba, S. D., Junker, M., Turner, L. D., and Scholten, R. E., “Mode stability of external cavity diode lasers,” *Appl. Opt.* **48**, 6692–6700 (Dec 2009).
- [6] Carr, A. V., Sechrest, Y. H., Waitukaitis, S. R., Perreault, J. D., Lonij, V. P. A., and Cronin, A. D., “Cover slip external cavity diode laser,” *Rev. Sci. Instrum.* **78**, 106108 (2007).
- [7] Cook, E. C., Martin, P. J., Brown-Heft, T. L., Garman, J. C., and Steck, D. A., “High passive-stability laser-diode design for use in atomic-physics experiments,” *Rev. Sci. Instrum.* **83**(4) (2012).
- [8] Talvitie, H., Merimaa, M., and Ikonen, E., “Frequency stabilization of a diode laser to doppler-free spectrum of molecular iodine at 633 nm,” *Opt. Comm.* **152**, 182–188 (1998).
- [9] Barrett, B., Carew, A., Beica, H. C., Vorozcovs, A., Pouliot, A., and Kumarakrishnan, A., “Prospects for precise measurements with echo atom interferometry,” *Atoms* **4**(3), 19 (2016).
- [10] Fukuda, K., Tachikawa, M., and Kinoshita, M., “Allan-variance measurements of diode laser frequency-stabilized with a thin vapor cell,” *Appl. Phys. B* **77**, 823–827 (2003).
- [11] Kunze, F., Wolf, S., and Rempe, G., “Measurement of fast frequency fluctuations: Allan variance of a grating-stabilized diode laser,” *Opt. Comm.* **128**, 269–274 (1996).